Fizeau's "aether-drag" experiment in the undergraduate laboratory

Thierry Lahaye and Pierre Labastie
Université de Toulouse, UPS, Laboratoire Collisions Agrégats Réactivité, IRSAMC; F-31062 Toulouse, France and CNRS, UMR 5589, F-31062 Toulouse, France

Renaud Mathevet
Université de Toulouse, UPS, Laboratoire Collisions Agrégats Réactivité, IRSAMC; F-31062 Toulouse, France; CNRS, UMR 5589, F-31062 Toulouse, France; and Laboratoire National des Champs Magntiques Intenses, UPR3228 CNRS/INSA/UJF/UPS, F-31400, Toulouse, France

(Received 16 December 2011; accepted 10 February 2012)

We describe a simple realization of Fizeau's "aether-drag" experiment. Using an inexpensive setup, we measure the phase shift induced by moving water in a laser interferometer and find good agreement with the relativistic prediction or, in the terms of 19th century physics, with Fresnel's partial-drag theory. This appealing experiment, particularly suited for an undergraduate laboratory project, not only allows a quantitative measurement of a relativistic effect on a macroscopic system but also constitutes a practical application of important concepts of optics, data acquisition and processing, and fluid mechanics.
[http://dx.doi.org/10.1119/1.3690117]

I. INTRODUCTION

In introductory courses and textbooks dealing with special relativity, Fizeau's "aether-drag" experiment often appears simply as an application of the law of composition of velocities, sometimes in the form of an exercise.[1] However, Albert Einstein himself declared that Fizeau's measurement of the speed of light in moving water was, together with stellar aberration, one of the experimental results that had influenced him most in the development of relativity.[2] In spite of this high praise, introductory expositions of Fizeau's experiment, including a discussion of its historical development and the details of the experimental setup, are often lacking. Moreover, many textbooks actually show incorrect experimental arrangements that would not allow for the observation of the effect in practice. Here, we show that one can actually perform Fizeau's experiment with rather modest equipment, and that such a project illustrates in an appealing way not only relativistic kinematics but also interesting aspects of wave optics, data acquisition and processing, and even fluid mechanics.

This article is organized as follows. We first review briefly the historical background of Fizeau's experiment, a "test" of special relativity carried out more than half a century before relativity was born! For completeness, we recall in Sec. III the derivation of the expected fringe shift in both the relativistic and non-relativistic frameworks, following the usual textbook treatment of the problem. We then turn to the main point of the paper, namely, how to reproduce the experiment in an undergraduate laboratory. Section IV is devoted to the description of our apparatus, starting with an emphasis on the experimental trade-offs one needs to address in the design phase. Finally, we discuss in Sec. V the results obtained, first with water as a moving medium and then with air, in order to discriminate between relativistic and non-relativistic predictions. The use of a white-light source instead of a laser is presented in Appendix A, with a discussion of the possible advantages and drawbacks. Appendix B establishes a useful fluid mechanics formula using dimensional analysis.

II. HISTORICAL BACKGROUND

Since Fizeau's aether-drag experiment is a landmark among the various experimental and theoretical developments leading to special relativity, it is worthwhile to recall briefly the history of these developments. An extensive historical study of the subject is beyond the scope of this paper. Here, we merely recall the main steps that led to Fizeau's aether drag experiment, as well as the major subsequent developments.[3]

We begin our reminder in the 17th century, at a time when the nature of light was a matter of harsh debate, as evidenced by the famous controversy between Christiaan Huygens and Isaac Newton. The speed of light in a vacuum c was known to be finite since the work of Ole Römer in 1676.[4] However, the measurement of the speed of light in a material medium of refractive index n was considered a crucial test because Huygens' wave theory implies that the speed of light in the medium is c/n, while Newton's corpuscular theory predicts it to be nc. Newton's views prevailed until the beginning of the 19th century, when interference experiments by Thomas Young and polarization experiments by Étienne Malus firmly established the wave theory.

An important event was the measurement by François Arago of the deviation of light from a distant star by a prism in 1810.[5] The idea of Arago is that if the speed of the light coming from distant stars is increased or decreased by the Earth's velocity, Newton's theory predicts that the deviation by a prism should be different from what would be observed if the source was terrestrial. He, therefore, tried to detect this difference and found a null result. This experiment seems to be the first in a long series that showed the impossibility of detecting the relative motion of light with respect to the Earth.[6]

Arago soon became friends with Augustin Fresnel, who had a mathematically sound theory of light waves, and asked him if the wave theory could explain the null result he had found. Fresnel's answer came a few years later.[7] His demonstration is based on the hypothesis of an absolute aether as a support of light waves, associated with a partial drag by transparent media. That is, if the medium of index n moves with speed $\boldsymbol{v}$, the aether inside the medium moves only at speed $\left(1-n^{-2}\right)\boldsymbol{v}$. The value of Fresnel's drag coefficient $1-n^{-2}$ precisely gives a null result for the Arago experiment. However, his demonstration, using some supposed elastic properties of the aether, is not so convincing by modern standards.[6]

The first Earth-based direct measurement of the speed of light was realized by Hippolyte Fizeau in 1849, by means of a rotating cogwheel. This kind of time-of-flight technique was soon improved by Léon Foucault who, using a rotating mirror, succeeded in showing that the speed of light is lower in water than in air.[8,9] Nevertheless, such *absolute* measurements were far from accurate enough to measure the small change of the speed of light in moving media.

This is where Fizeau's aether-drag experiment enters the scene. As we shall see, this experiment is based on a much more sensitive *differential* measurement using the interferometric arrangement shown in Fig. 1. The experiment was performed in 1851 and almost immediately reported to the French academy of science, and then translated into English.[10] Fizeau measured an effect in agreement with Fresnel's theory to within a few percent, which unambiguously ruled out concurrent theories postulating total aether drag.

Many experiments of increasing precision were then undertaken to try to demonstrate the influence of Earth's motion on light propagation, but all gave null results. It soon became apparent that Fresnel's partial drag did not allow the measurement of any absolute motion of Earth to first order in v/c. In what would now be called a review paper,[11] Éleuthère Mascart concludes in 1874 (our translation): "the general conclusion of this memoir would be […] that the translation motion of the Earth is of no appreciable consequence on optical phenomena produced with terrestrial sources or solar light, that those phenomena do not allow to appreciate the *absolute* motion of a body and that only *relative* motions can be attained."

In 1881 Albert Michelson designed a new interferometer, which, according to existing theories, could detect Earth's displacement respective to aether because the expected effect was proportional to $(v/c)^2$. His first measurement was at most half of the expected fringe shift. He then improved the apparatus with Edward Morley. The two physicists gradually became convinced of a null result. In 1886 they decided to redo Fizeau's experiment—the only experiment with a positive result, and one that had yet to be reproduced. With a careful design of the hydraulics and an improved design for the interferometer,[12] they confirmed Fizeau's result, and Fresnel's aether drag, with much higher precision. However, in their celebrated experiment of 1887,[13] the measured shift was at most 0.01 fringe instead of an expected 0.4. The two experiments were thus incompatible according to existing theories, Fizeau's needing a partial drag and Michelson-Morley's needing a total drag of aether.

History then accelerated. In the late 1880 s, George Fitzgerald proposed the concept of length contraction. In 1895, Hendrick Lorentz published his theory of electromagnetic media, in which he derived Fresnel's formula from first principles. At the beginning of the 20th century, it became evident that time dilation was also necessary to account for all electromagnetic phenomena. After Albert Einstein published the theory of special relativity in 1905, Max Laue, in 1907, derived Fresnel's drag coefficient from the relativistic addition of velocities.[14] All experiments, being either of first (Fizeau) or second (Michelson-Morley) order in v/c, were then explained by a single theory with no need for an aether with such special properties.

In the relativistic framework, one can also account for the effects of dispersion, already predicted by Lorentz in 1895. Although the supplementary term makes only a few percent correction, Pieter Zeeman, in his 1914–1927 experiments, succeeded in measuring it.[15,16] More recently, this experiment was performed in liquids, solids, and gases using ring lasers[17] and confirmed the value of the dispersion term to within 15%.[18] Fizeau's experiment has also been successfully transposed to neutron matter waves.[19]

Thus, as may not be commonly understood, Fizeau's aether-drag experiment was a crucial turning point between old and modern conceptions of light and space-time. We believe this makes its replication particularly valuable from a pedagogical point of view.

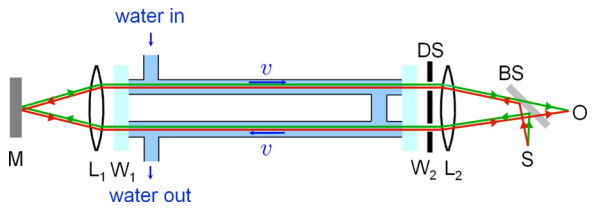

Fig. 1. (Color online) Sketch of the interferometer used by Fizeau (adapted from Michelson, Studies in Optics. Copyright © 1995 by Dover). For the sake of clarity, the two counter-propagating beams are drawn in different gray levels (colors). *S*: source; *O*: observer; *M*: mirror; W_i: windows; L_i: lenses; *BS*: beam splitter; *DS*: double slit.

III. THEORETICAL BACKGROUND

In this section, we recall the derivation of the phase difference $\Delta\varphi$ induced by the motion, with velocity v, of the medium of refractive index n in the interferometric arrangement shown in Fig. 2, which is essentially the one used by Michelson and Morley in 1886.[12] Let us consider first the case where water and monochromatic light of vacuum wavelength λ propagate in the same direction [shown as light gray (green online) in Fig. 2]. In the reference frame where water is at rest, the phase velocity of light is c/n. In the laboratory frame, using the relativistic composition of velocities, the phase velocity of light is

$$v_+ = \frac{c/n + v}{1 + (v/n)/c^2} = \frac{c/n + v}{1 + v/(nc)}. \tag{1}$$

The phase accumulated by light over the propagation distance of 2ℓ is thus

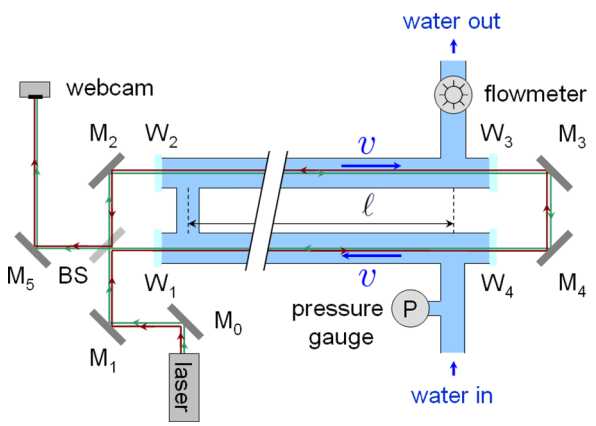

Fig. 2. (Color online) Sketch of the experimental setup (see text for details). M_i: mirror; W_i: windows; *BS*: beam splitter. The two counter-propagating beams are drawn in different gray levels (colors) for clarity.

$$\varphi_+ = \frac{2\pi c}{\lambda}\frac{2\ell}{v_+}. \tag{2}$$

Where light and water propagate in opposite directions [shown as dark gray in Fig. 2], the corresponding phase φ_- is obtained by replacing v by $-v$ in Eq. (1). The phase difference between the two arms of the interferometer thus reads

$$\Delta\varphi = \varphi_- - \varphi_+ \tag{3}$$

$$= 2\pi\frac{2\ell c}{\lambda}\left(\frac{1 - v/(nc)}{c/n - v} - \frac{1 + v/(nc)}{c/n + v}\right). \tag{4}$$

Expanding the above result to first order in v/c, we find

$$\Delta\varphi_{\text{rel.}} = 2\pi\frac{v}{c}\frac{4\ell}{\lambda}\left(n^2 - 1\right). \tag{5}$$

It is not difficult to perform the same calculation using the non-relativistic addition of velocities, i.e., by replacing $v_\pm$ by $c/n \pm v$. One then finds

$$\Delta\varphi_{\text{non-rel.}} = 2\pi\frac{v}{c}\frac{4\ell}{\lambda}n^2, \tag{6}$$

which has the same functional form except for a coefficient n^2 in place of $n^2 - 1$. In Fresnel's language, this would correspond to a complete aether-drag. The ratio of the predictions [Eqs. (6) and (5)] is about 2.3 for water ($n \simeq 1.33$) and approximately 1700 for air ($n \simeq 1.0003$), whence the interest in performing the experiment with air in addition to water (see Sec. V E).

As previously mentioned, the above derivation was first carried out by Laue in 1907[14] and is the one found in most textbooks. It has been pointed out[16] that such an approach is not strictly valid because the relativistic composition of velocities applies to point-like particles, and not to the phase velocity of waves. However, a more rigorous derivation, based on the Lorentz transformation of the four-vector $k^\mu = (\omega/c, \boldsymbol{k})$ associated with light, gives the same result provided the light and the medium propagate along the same axis.[16]

Up until now, we have neglected dispersion, i.e., the variation of the refractive index of the moving medium with the frequency of light ω. But the frequency of light in a moving frame is shifted by the Doppler effect. These shifts are opposite for the counterpropagating beams in the interferometer. They are then subjected to slightly different refraction indices due to dispersion. Taking this into account, the factor $n^2 - 1$ in Eq. (5) must to be replaced by[20]

$$n^2 - 1 + n\omega\frac{\mathrm{d}n}{\mathrm{d}\omega}. \tag{7}$$

Using the wavelength-dependent refractive index of water found in tables,[21] a simple calculation shows that for water at $\lambda = 532\,\text{nm}$, the fringe shift is actually 3.8% greater than what Eq. (5) predicts.

IV. EXPERIMENTAL SETUP: FIZEAU'S EXPERIMENT MADE EASY

A. Requirements

Fizeau's experiment was a real tour de force made possible by the very clever design of the experiment (see Fig. 1). The improvement by Michelson and Morley essentially transforms the original wavefront-division setup into a much brighter amplitude-division setup. In both arrangements, which we would now call Sagnac interferometers,[22] the two interfering beams follow almost exactly the same path (see Fig. 2). This not only doubles the interaction length with the moving medium, but more importantly, rejects common-mode phase fluctuations due, for example, to turbulence. This arrangement also ensures that the optical path length difference between the two interfering arms is zero when the interferometer is perfectly aligned.

Equation (5) shows that the expected fringe shift is enhanced by using a short wavelength λ and a large product ℓv. Let us estimate the requirements of the water velocity. We first set $\ell \sim 2\,\text{m}$ to make the size of the apparatus reasonable. Next, we choose $\lambda = 532\,\text{nm}$ to correspond to inexpensive diode-pumped solid-state lasers. We then see that achieving a phase shift on the order of 1 rad using water ($n \simeq 1.33$) requires velocities on the order of 4 m/s. The experimental setup thus requires that we can detect a phase shift of a fraction of a fringe and to produce a water flow of several meters per second.

The key to the success of the experiment is the care taken when setting up the plumbing. We thus describe in detail the various components of our experimental setup and refer the reader to the pictures shown in Fig. 3.

B. Hydraulics

For simplicity and to keep costs low, we built our system from standard piping materials available in any hardware store, and such that a regular tap can be used for the water source. Ideally, a large diameter d of the pipes is desirable because it simplifies the alignment of the interferometer beams and improves the velocity profile flatness over the beam section. However, the volumetric flow rate $Q = \pi d^2 v/4$ increases rapidly with d (for fixed v). The typical maximal flow rates available at the water outlets of a laboratory are on the order of 10–20 l/min. To achieve a velocity of $v \sim \text{m/s}$ thus requires $d \lesssim 10$ mm. Although using smaller-diameter pipes will lead to a higher flow velocity, it becomes impractical for the alignment of the laser beams and leads to increased head loss. The flow rate is, therefore, limited by the pressure available from the water distribution system. Unfortunately, the use of a pump to increase the inlet pressure is of little help because in the turbulent regime, which is relevant here, the flow rate increases only as the square root of the pressure (see Fig. 4 and Appendix B). In our experiment, we use 8-mm inner diameter copper tubing, allowing us to reach $v \sim$ m/s.

The water pressure ΔP is varied using the tap valve and measured with a pressure gauge connected to the inlet port (see Fig. 2). We get a continuous measurement of the flow rate Q using a paddlewheel flowmeter[23] that delivers a square electric signal, whose frequency depends linearly on the flow rate. Flowmeter calibration, reported in the inset of Fig. 4, was realized by measuring the volumetric flow rate Q of water through the system with a graduated bucket and a stopwatch. We estimate the accuracy of our crude flow rate calibration to be on the order of 5%. With moderate effort, a calibration at the percent level or better could certainly be achieved. Note that the velocity $v_{\text{meas}} = 4Q/(\pi d^2)$ measured in this way is the mean velocity averaged over the radial velocity profile inside the pipes, and *not* the velocity v

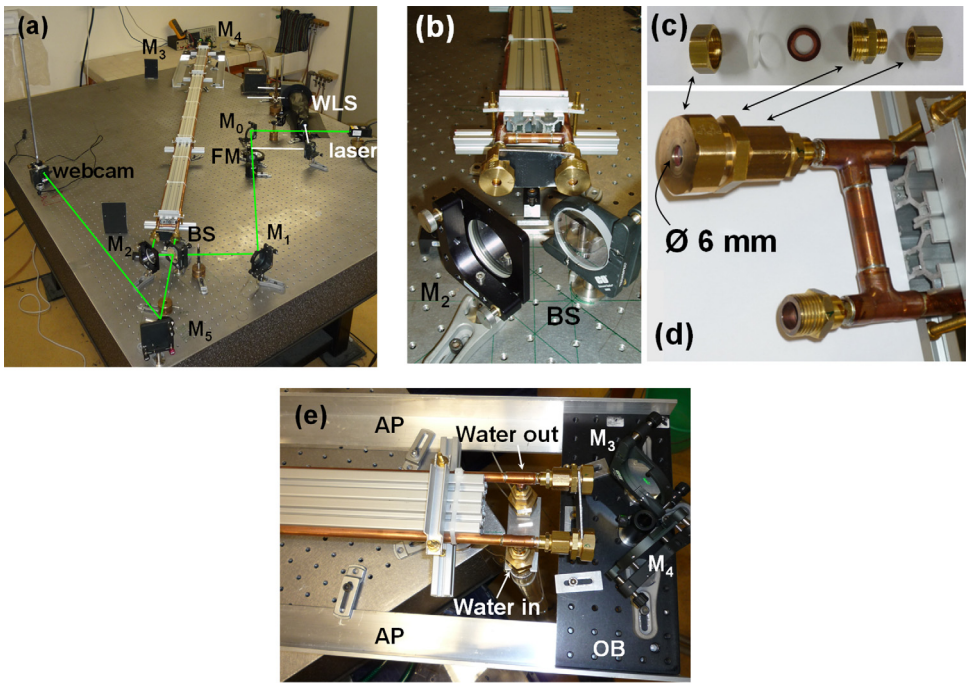

Fig. 3. (Color online) (a) General view of the experimental setup. WLS: white-light source; FM: flipping mirror. (b) Close-up of one end of the interferometer. (c) The various parts for connecting a window, from left to right: drilled brass BSP blank, BK7 25-mm diameter window, gasket, BSP reducer, BSP adapter. (d) Close-up of the interferometer end shown in (b), with one window disconnected. (e) The other end of the interferometer, showing the water connections and the optical breadboard (OB) supporting mirrors M_3 and M_4. AP: aluminum profiles.

appearing in Eq. (5) that occurs at the position of the beam. We will discuss this point in more detail below.

C. Mechanics

The two 2-m long copper pipes are relatively flexible and soft. Their straightness and parallelism are ensured by fastening them on a slotted, 30×60 mm^2 cross-section aluminum profile by means of cable ties [see Fig. 3(b)]. The T-shaped connections at their ends [see Figs. 3(d) and 3(e)] are made with low melting point tin solder and a heat gun. On the four ends where the windows need to be installed, male 3/8 in. British Standard Pipe (BSP) adapters are soldered.

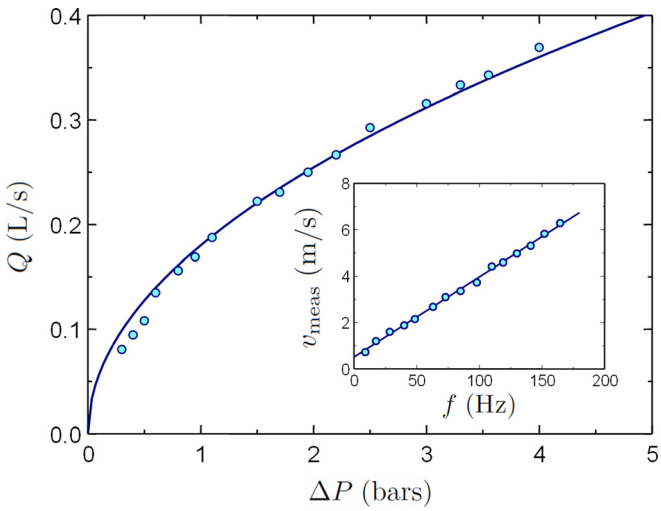

Fig. 4. (Color online) Flow rate Q through the apparatus as a function of the head loss ΔP. The solid line is a fit by the function $Q = a\sqrt{\Delta P}$ with a as an adjustable parameter; the best fit gives $a \simeq 0.18\,\mathrm{L}/(\mathrm{sbar}^{1/2})$. Inset: calibration curve of the flowmeter allowing one to infer the water speed v_{meas} from the frequency f of the signal it delivers. The solid line is the result of a linear fit.

The windows themselves are 3.3-mm thick, 25-mm diameter uncoated borosilicate glass substrates.[24] They are attached to the pipes via the system shown in Figs. 3(c) and 3(d). The window is pressed against a brass female 3/4 in. BSP cap at the center of which a 6-mm diameter hole is drilled. The inner threads were slightly altered with a lathe to fit the window outer diameter. The cap and window are then tightened with a fiber gasket onto a male–male BSP 3/4 in. to 3/8 in. adapter which is itself connected to the male BSP adapter soldered to the pipe via a female–female 3/8 in. BSP adapter.

The end with hoses connected to the water inlet and outlet in the laboratory sink is extended over the side of the table [see Fig. 3(e)]. Two L-shaped aluminum profiles mounted on the table support a small piece of optical breadboard on which we mount the two mirrors M_3 and M_4. In a preliminary set of experiments, we tried a configuration in which the water pipes were supported independently from the optical table (and thus from the interferometer) in order to avoid possible detrimental vibrations. However, this turned out to be cumbersome, and the much simpler solution of clamping the pipes tightly to the optical table, by means of four regularly spaced post-holders, does not yield any degradation of the measurements.

D. Optics and alignment

As a light source, we use an inexpensive diode-pumped, solid-state laser delivering a quasi-collimated beam with several milliwatts of light at $\lambda = 532$ nm.[25] The metallic mirrors (M_{0-4}) and the dielectric beamsplitter are all mounted on kinematic optical mounts. We found it convenient to draw the light path directly on the optical table [see Fig. 3(b)]

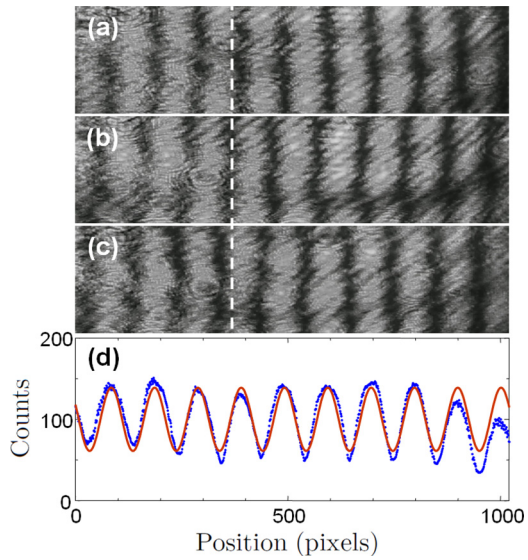

Fig. 5. (Color online) Sample images of the fringe pattern obtained from the camera for (a) $v=-5.7$ m/s, (b) $v=0.8$ m/s, and (c) $v=5.7$ m/s. The white dashed line shows the position x_0 of the central fringe for $v=0$. (d) Processing of the image shown in (c)—the dots are the vertically integrated intensities and the (red) solid curve is the best fit to Eq. (8).

before mounting the mirrors and the beamsplitter, as this considerably simplifies the alignment of the interferometer.

To align the interferometer, we begin with four small diaphragms (diameter ~2 mm) positioned just in front of the centers of the windows W_{1-4}. The tubing system is then removed, and one walks the beam using M_1, BS, and M_2 so that beams W_1W_4 and W_2W_3 pass through the diaphragms. Using M_3 and/or M_4, one then aligns the returning beam onto the incoming one. After a few iterations, one obtains a quasi-perfect superposition of the beams and observes an almost flat intensity profile in the interference field. When tilting slightly one of the mirrors (e.g., M_3), nice straight parallel fringes appear.

Now the pipes can be repositioned and clamped onto the table. Water is set to flow, and one makes sure that no air bubbles are trapped inside the pipes, especially close to the windows where the diameter is larger. If so, they can be removed by loosening the cap while the water is flowing.

Instead of the expected fringe pattern, one usually observes caustics and diffuse reflections on the inner sides of the pipes. Indeed, due to the soldering, the parallelism of the windows cannot be ensured. When a beam strikes the window at a small angle from the normal, its path is slightly deviated. This deviation is only partially compensated at the inner glass/water interface, so the interferometer must be realigned. After a few iterations, the fringes return (see Fig. 5).

V. EXPERIMENTAL RESULTS

A. Data acquisition

For quantitative measurements of the fringe shift, we use an inexpensive webcam,[26] whose objective lens and IR filter have been removed in order to directly expose the CMOS detector chip to the fringe pattern. Using the micrometer screws of mirror M_2, for instance, the fringes are set parallel to one of the axes of the camera chip. From the webcam software, the gamma correction is adjusted to get a linear response of the detector.[27] The integration time and light intensity are adjusted to use the full dynamic range of the webcam, taking care not to saturate any pixels.

An important point for later data processing is that, prior to acquiring a series of images, one needs to locate the position of the central fringe on the camera. For this, it is convenient to wobble mirror M_2, for example. The fringe spacing varies, and the fringes move symmetrically away from the central one which is dark and does not move. Once the position x_0 of the central fringe has been located, the webcam is roughly centered on it to limit systematic errors due to changes in the fringe spacing. The fringe spacing is then adjusted to get about ten fringes on the detector chip. Too few fringes will not allow for an accurate measurement of the fringe position offset and period. On the other hand, if the fringes are too narrow, the resolution of the camera will limit accuracy.

B. Data processing

We process the images in the following way. We sum up the values of all pixels in a column, and thus obtain a one-dimensional intensity distribution $I(x)$, where x (in pixels) denotes the position along an axis perpendicular to the fringes (see Fig. 5). We then fit the data using

$$I(x) = I_0 + I_1 \sin\left(\frac{2\pi(x-x_0)}{\Lambda} + \Delta\varphi\right), \tag{8}$$

where I_0, I_1, Λ, and $\Delta\varphi$ are adjustable parameters, and x_0 is the (fixed) position of the central fringe, determined as explained above.

C. Experimental results with water

Acquisition and processing are repeated for various water velocities. Figure 6 shows the experimentally measured phase difference $\Delta\varphi$ as a function of the measured water velocity v_{meas}. The origin of phases has been chosen to vanish at zero velocity. As can be seen in the figure, we take five measurements for each velocity to improve the statistics and to get an estimate of the variance. Negative velocities were

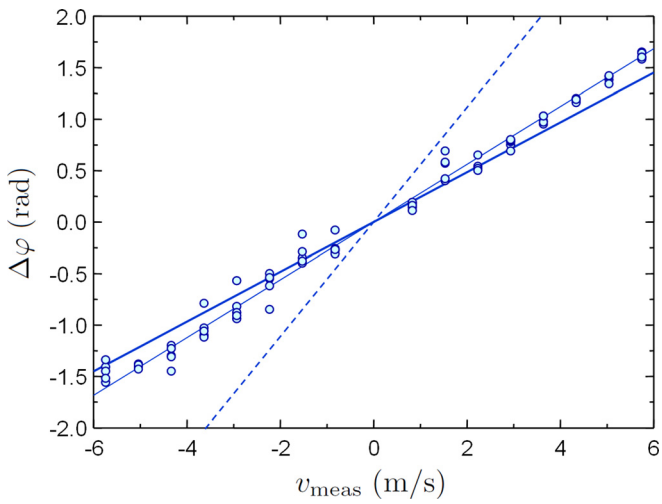

Fig. 6. (Color online) Experimental results using water as the moving medium. Circles: data; thin solid line: linear fit, giving a slope of 0.274 ± 0.003 rad s/m; thick solid line: relativistic prediction from Eq. (5); dashed line: non-relativistic prediction from Eq. (6).

obtained simply by exchanging the inlet and outlet ports of the tubing system. No data could be recorded for velocities below 1 m/s. Indeed, when the velocity is low, turbulence in the pipes is not fully developed, which leads to low spatial and temporal frequency fluctuations and very unstable pictures. We also could not take data for zero velocity because in this case the inlet or outlet valve must be closed; such a situation produces undue stress on the tubing system so that light can no longer properly exit the system. For this reason, the alignment procedure must be performed with water flowing in the pipes.

We observe a clear linear dependence of $\Delta\varphi$ on v_{meas}. A linear fit (thin solid line) gives a slope of 0.274 ± 0.003 rad s/m. The non-relativistic prediction of Eq. (6) (dashed line) has slope 0.563 rad s/m, which does not match the experimental results at all. The relativistic prediction given by Eq. (5) (thick solid line) has slope 0.248 rad s/m and is in much better agreement with the experimental data. However, there appears to be a slight systematic error in the data compared with the prediction. As stated earlier, this comes from the fact that we measure the mean velocity v_{meas} averaged over the velocity profile inside the pipes, whereas the velocity v appearing in Eq. (5) is the velocity at the position of the beam, i.e., on the axis of the pipes.

To understand how v_{meas} is related to v, let $v(r)$ denote the radial dependence of the velocity in the pipes of radius R and let $v_{\max} = v(0)$. Because the beam is well centered on the pipe by construction, we can safely assume that $v = v_{\max}$. We must therefore multiply the theoretical prediction by the correction factor

$$\frac{v_{\max}}{v_{\text{meas}}} = \frac{\pi R^2 v_{\max}}{\int_0^R 2\pi r v(r) \mathrm{d}r}. \tag{9}$$

A theoretical model for the radial dependence $v(r)$ is thus required. In the laminar regime (Poiseuille flow), $v(r)$ would have the parabolic shape shown as the dashed curve in Fig. 7, which, using Eq. (9), gives a correction factor equal to 2. However, for $v \gtrsim 1$ m/s, one can check that the Reynolds number $\mathrm{Re} = vd/\nu \gtrsim 10^4$, making the flow turbulent. Here, $\nu \sim 10^{-6}\mathrm{m}^2/\mathrm{s}$ denotes the kinematic viscosity of water. Under these conditions, there is no simple rigorous analytic expression for the velocity profile. However, for the range of Reynolds numbers used here, experimentally measured flow profiles are well reproduced[12] by the empirical law $v(r) = v_{\max}(1 - r^2/R^2)^{1/6}$, corresponding to the much flatter velocity profile shown as the solid curve in Fig. 7. In the turbulent regime, Eq. (9) then gives a correction factor of 1.16. The relativistic prediction (5) multiplied by this correction factor, and including the 3.8% correction due to dispersion, yields a slope of 0.299 rad s/m (not shown in Fig. 6). The agreement between the experimental and theoretical values is thus at the level of 8%.

D. Discussion

Based on our data, we conclude that the non-relativistic prediction is clearly ruled out by our measurements. Nevertheless, the rather good agreement with the relativistic prediction must not be over interpreted. Indeed, it is difficult to put an accurate error bar on the result, as several systematic effects should be studied carefully for such a purpose. First, the systematic errors are dominated by our flowrate measurement. A more careful calibration should thus be performed in order to improve the accuracy. Second, the factor of 1.16 due to the shape of the velocity profile should be measured specifically for our system. A final source of uncertainty is the determination of the actual length ℓ appearing in Eq. (5). In practice, the flow makes a right-angle turn at each end of the pipes, so the velocity will presumably be affected up and downstream on length scales on the order of the pipe diameter d. This implies a correction of order d/ℓ (on the percent level), but again, an accurate estimation is difficult.

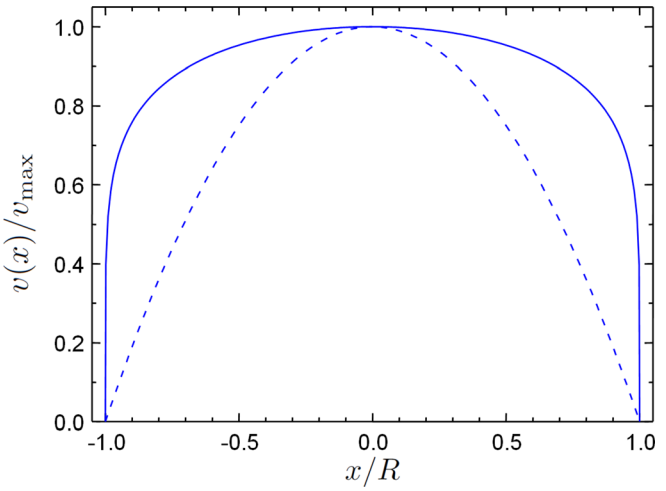

Fig. 7. (Color online) Dashed curve: Poiseuille's velocity profile for laminar flow given by $v(r) = v_{\max}(1 - r^2/R^2)$. Solid curve: velocity profile for turbulent flow, modeled here by the empirical form $v(r) = v_{\max}(1 - r^2/R^2)^{1/6}$.

In the end, due to a slight distortion of the tubing when the velocity (and thus the pressure) is varied, the fringe spacing changes by a small amount. As mentioned, an important feature of the Sagnac-like interferometric arrangement used here is that it operates at low interference order p. This is crucial in order to be sure that when the water is flowing inside the pipes, the observed shift of the fringes does arise from the aether drag effect and not from a slight change in the fringe spacing. As an example, let us assume that using a different interferometric setup, one observes an interference pattern with ten fringes, corresponding to interference orders, say $p_1 = 10^4$ to $p_2 = p_1 + 10$. If, as is likely, the fringe spacing changes by a quantity as small as 10^{-4} in relative value when the water velocity varies, one would observe that our ten fringes would shift, almost as a whole, by as much as one full fringe! For the data presented in the paper, we have measured that the fringe period Λ does not vary by more than 5% over the full range of velocities, yielding negligible errors due to the low interference orders used here.

E. Experimental results with air

In his original paper,[10] Fizeau states that he performed the experiment with air as a moving medium and that "the motion of the air does not produce any sensible displacement of the fringes," in agreement with the partial drag prediction (5). On the contrary, the non-relativistic prediction (6) predicts a measurable shift.

It is thus interesting to repeat the experiment using air instead of water. We do so by using a standard compressed air outlet, as available in most laboratories. One actually needs very moderate pressures in order to achieve relatively

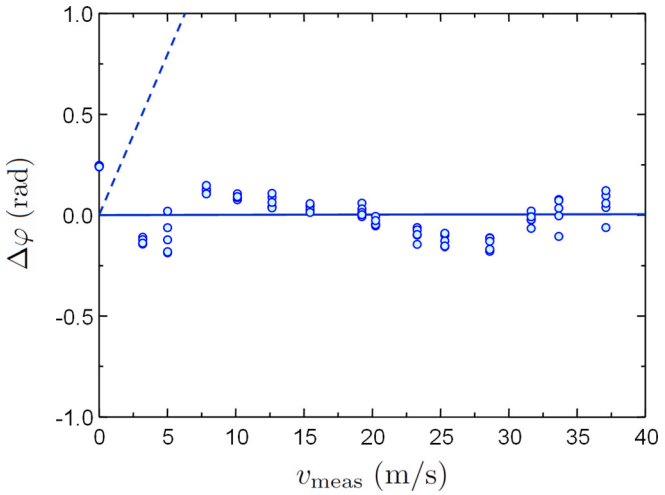

Fig. 8. (Color online) Experimental results using air as the moving medium. Circles: data; solid line: relativistic prediction from Eq. (5); dashed line: non-relativistic prediction from Eq. (6).

high velocities for the air flow in the 8-mm diameter pipes: only 0.2 bar typically yields $v_{\mathrm{meas}} \simeq 35\mathrm{m/s}$. Measuring the air velocity is not as straightforward as with water; we found it convenient to use a hot-wire anemometer[28] placed in a $D = 18$ mm inner-diameter pipe at the outlet of the $d = 8$ mm pipes. The velocity v_{meas} in the interaction region of the interferometer is then deduced from the measured velocity v_{anem} at the anemometer position via volumetric flow conservation $v_{\mathrm{meas}} = v_{\mathrm{anem}}(D/d)^2$. This assumes incompressible flow, which is valid since the air velocity is much smaller here than the speed of sound.[29]

Figure 8 shows the measured phase shifts (circles) along with the predictions of Eqs. (5) and (6). We cannot clearly identify the reason(s) behind the seemingly oscillatory behavior of the measured fringe shift with velocity. In any case, the non-relativistic prediction is clearly ruled out by the measurements, which are clearly compatible with the relativistic calculation.

VI. CONCLUSION AND OUTLOOK

Using rather modest equipment, we have shown that Fizeau's "aether-drag" experiment can be reproduced in the undergraduate laboratory at a quantitative level. It not only makes a nice practical introduction to the sometimes abstract concepts of special relativity but also constitutes an interesting application of several branches of experimental physics.

Immediate improvements of the setup described in this paper would consist of (i) calibrating the flowrate more carefully and (ii) increasing the stiffness of the tubing system. A natural extension of this work, suitable for a long-term student project, would consist of trying to study the systematic effects in detail—for example, the determination of the effective length ℓ. One way to measure this effect would be to start from the full pipe length and then repeat the experiment for shorter and shorter pipe lengths. The effect can then be evaluated by measuring the dependence of the slope $\Delta\varphi/v$ on the pipe length.

A more ambitious extension, suitable for advanced undergraduates, would illustrate more modern optical techniques. For instance, one may use a ring cavity of moderately high finesse (say $\mathcal{F} \sim 100$ –1000) and measure the variation of the resonance frequencies of the two counterpropagating modes when the velocity of the medium is varied. A gain in sensitivity by a factor $\mathcal{F}$ is then expected. Such techniques, with ultra-high finesse cavities, are currently used to measure, for example, non-reciprocity effects in the propagation of light with amazing sensitivities.[30]

ACKNOWLEDGMENTS

The authors thank Éric Desmeules for instigating this project and his students Mélodie Andrieu and Laurane Boulanger for help in setting up a preliminary version of the apparatus during their "TIPE" project (the data shown in Figs. 4 and 6 were essentially acquired by them). The authors thank Jacques Vigué for useful discussions. David Guéry-Odelin created the conditions that made this project possible. R.M. dedicates his contribution to José-Philippe Pérez for inspiring discussions over the years. Funding by CNRS is acknowledged.

APPENDIX A: USING A WHITE-LIGHT SOURCE INSTEAD OF A LASER

We have also performed this experiment using a white-light source instead of a laser. The source is a 1-mm diameter iris illuminated by a 55-W halogen lamp (the type used for car headlights) and a condenser lens. The resulting diverging beam is collimated by a 100-mm focal length lens and superimposed onto the path of the laser beam using two mirrors. The second mirror, located between M_0 and M_1, is a flipping mirror so that one can switch easily between the laser and the white light sources [see Fig. 3(a)]. Once the interferometer has been aligned with the laser, white-light fringes are readily observed. Naturally, if the iris is opened the luminosity is increased at the expense of spatial coherence, and the contrast in the picture is lost. The fringes are then localized in the vicinity of mirror M_3. A color image as in Fig. 9(a) is then recovered using a converging lens that conjugates M_3 and the detector plane.

The advantages of using a white source is that (i) the position of the dark central fringe can be found without ambiguity as the contrast of the colored fringes vanishes rapidly away from the zero path-length difference and (ii) compared to using a laser, unwanted interference fringes (due to scattering on dust particles for example) as well as speckle, are suppressed. There are,

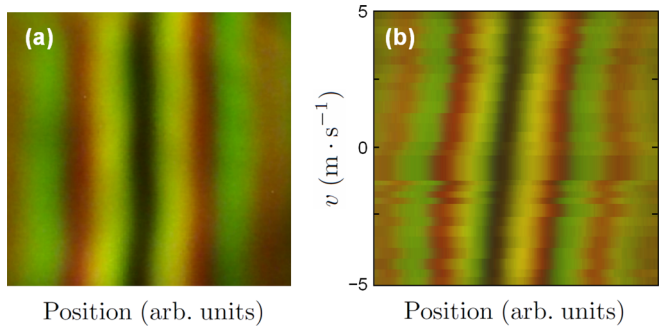

Fig. 9. (Color online) (a) A sample white-light fringe pattern. (b) Composite image of 22 fringe patterns obtained for different water velocities v. One clearly observes the linear shift of the central fringe position as a function of v.

however, a certain number of drawbacks. Besides the reduced luminosity, making quantitative comparisons with theory is obviously much more difficult than in the monochromatic case. Indeed, one would need to measure the light spectrum, as well as the wavelength-dependent reflectivity (including phaseshifts) introduced by the beamsplitter in order to model quantitatively the fringe pattern. For instance, we have observed that using a metallic beamsplitter instead of the dielectric one significantly alters the colors and the contrast of the fringe pattern obtained in white light.

We made a composite of 22 images taken for various water velocities v. The result, shown in Fig. 9(b), clearly shows that the fringe positions shift linearly with velocity. However, a quantitative analysis of such an image is not easy, and the motivation behind this figure is mainly for aesthetics.

APPENDIX B: TURBULENT HEAD LOSS IN A CIRCULAR PIPE: DIMENSIONAL ANALYSIS APPROACH

In the standard introductory physics curriculum, the computation of the head loss in a circular pipe is done using Poiseuille's equation, valid for laminar flow. It is much less common to present the case of turbulent flow to undergraduate students. Reference to the Moody diagram, giving the so-called *friction factor* as a function of Reynolds number and pipe roughness, can be found in engineering-oriented textbooks, but may appear as quite involved to beginning physics students. In this appendix, we show how dimensional analysis can be used to infer a plausible expression for the turbulent head loss, at least for its dependence on flow rate and pipe diameter, two parameters that are crucial for the design of our experimental setup.

We consider the head loss ΔP for the flow of a fluid of density ρ and kinematic viscosity ν in a circular pipe of diameter d and length l, flowing with a volumetric flow rate Q. Let us make two assumptions. First, for an infinitely long pipe, only the pressure gradient $\Delta P/l$ is physically relevant. And second, the limit of very large Reynolds number corresponds formally to the limit $\nu \to 0$. In this case, the viscosity ν should not appear explicitly in the expression for the head loss. Under these conditions, we expect the functional form for the head loss to be

$$\frac{\Delta P}{l} = A\rho^{\alpha}Q^{\beta}D^{\gamma}, \tag{B1}$$

where A is a dimensionless constant and (α, β, γ) the exponents to be determined. Equating the dimensions on both sides of this equation yields three equations for the exponents, which can be solved to give

$$\frac{\Delta P}{l} = A\frac{\rho Q^2}{D^5}. \tag{B2}$$

This expression agrees well with empirical formulae used in an engineering context if one chooses $A \sim 3 \times 10^{-2}$, and this is typically what one would find using the friction factor obtained in a Moody diagram[31,32] for our Reynolds numbers. For example, the value of the coefficient a obtained when fitting the flow rate data of Fig. 4 yields $A \simeq 2.5 \times 10^{-2}$, in good agreement with the previous estimate.

[1]E. F. Taylor and J. A. Wheeler, *Spacetime Physics: Introduction to Special Relativity*, 2nd ed. (W. H. Freeman & Company, New York, 1992).
[2]R. S. Shankland, "Conversations with Albert Einstein," Am. J. Phys. **31**, 47–57 (1963).
[3]For a detailed account, see O. Darrigol, "The genesis of the Theory of Relativity," Séminaire Poincaré, **1**, 1–22 (2005), available online at www.bourbaphy.fr/darrigol2.pdf, and references therein.
[4]O. Römer, "Démonstration touchant le mouvement de la lumière trouvé par M. Romer de l'Académie Royale des Sciences," J. des Sçavans, 233–236 (1676). An English translation appeared quickly in Philos. Trans. **12**, 893–894 (1677), available online at http://dx.doi.org/10.1098/rstl.1677.0024.
[5]Arago gave an account of the results to the French Academy of Sciences, but the text was not published until 1853, in F. Arago, "Mémoire sur la vitesse de la lumière," C. R. Acad. Sci. **36**, 38–49 (1853), available online at http://gallica.bnf.fr/ark:/12148/bpt6k2993z/f42.image.
[6]For a modern account see R. Ferraro and D. M. Sforza, "Arago (1810): The first experimental result against the ether," Eur. J. Phys. **26**, 195–204 (2005).
[7]A. Fresnel, "Lettre de M. Fresnel à M. Arago, sur l'influence du mouvement terrestre dans quelques phénomènes d'optique," Ann. Chim. Phys. **9**, 57–66 (1818), available online at http://www.google.com/books?id=nZc5AAAAcAAJ.
[8]L. Foucault, *Sur les vitesses relatives de la lumière dans l'air et dans l'eau* (Bachelier, Paris, 1853), available online at http://www.bibnum.education.fr/files/foucault-texte.pdf.
[9]A. A. Michelson, *Studies in Optics* (Dover, New York, 1995).
[10]H. Fizeau, "Sur les hypothèses relatives à l'éther lumineux, et sur une expérience qui paraît démontrer que le mouvement des corps change la vitesse avec laquelle la lumière se propage dans leur intérieur," C. R. Acad. Sci. **33**, 349–355 (1851); translated into English in H. Fizeau, "On the effect of the motion of a body upon the velocity with which it is traversed by light," Philos. Mag. 4th series **2**, 568–571 (1851). A longer account, with the same title, was published in H. Fizeau, Ann. Chim. Phys. **57**, 385–404 (1859), and translated in H. Fizeau, Philos. Mag. 4 th series **19**, 245–260 (1860).
[11]É. Mascart, "Sur les modifications qu'éprouve la lumière par suite du mouvement de la source lumineuse et du mouvement de l'observateur," Ann. Sci. Ec. Normale Super. (2 nd series) **3**, 363–420 (1874), available online at http://www.numdam.org/numdam-bin/feuilleter?j=asens.
[12]A. A. Michelson and E. W. Morley, "Influence of Motion of the Medium on the Velocity of Light," Am. J. Sci. **31**, 377–386 (1886).
[13]A. A. Michelson and W. Morley, "On the relative motion of the Earth and the luminiferous ether," Am. J. Sci. **34**, 333–345 (1887).
[14]M. Laue, "Die Mitführung des Lichtes durch bewegte Körper nach dem Relativitätsprinzip," Ann. Phys. **328**, 989–990 (1907).
[15]P. Zeeman, "Fresnel's coefficient for light of different colors (first part)," Proc. Roy. Acad. Sci. Amsterdam **17**, 445–451 (1914); "Fresnel's coefficient for light of different colours (second part)," *ibid.* **18**, 398–408 (1915). This experiment was recently revisited by Lerche who claims, on the basis of ignored systematic effects, that Zeeman's experiments are inconclusive.[16]
[16]I. Lerche, "The Fizeau effect: Theory, experiment, and Zeeman's measurements," Am. J. Phys. **45**, 1154–1164 (1977).
[17]W. M. Macek, J. R. Schneider, and R. M. Salamon, "Measurement of Fresnel Drag with the Ring Laser," J. Appl. Phys. **35**, 2556–2557 (1964).
[18]H. R. Bilger and A. T. Zavodny, "Fresnel Drag in a Ring Laser: Measurement of the Dispersive Term," Phys. Rev. A **5**, 591–599 (1972).
[19]A. Klein et al., "Neutron Propagation in Moving Matter: The Fizeau Experiment with Massive Particles," Phys. Rev. Lett. **46**, 1551–1554 (1981).
[20]J. D. Jackson, *Classical Electrodynamics*, 3rd ed. (Wiley, New-York, 1998), chap. 11.
[21]P. Schiebener, J. Straub, J. M. H. Levelt Sengers, and J. S. Gallagher, "Refractive index of water and steam as function of wavelength, temperature and density," J. Phys. Chem. Ref. Data **19**, 677–717 (1990).
[22]E. Hecht, *Optics*, 4th ed. (Addison-Wesley, San Franciso, 2002), pp. 412–413.
[23]Gems sensors rotoflow 155421 BSPP-RS.
[24]Edmund Optics, model 43892.
[25]Shangai Dream Lasers SDL-532-005T.
[26]Philips SPZ5000 webcam.
[27]This linearity can be checked by using a powermeter (or a calibrated photodiode) and a set of neutral density filters to attenuate the laser beam.

One then readily verifies that for a proper setting of the webcam's *gamma*, the pixel counts are proportional to the light intensity on the detector.

[28]Testo 425 hot-wire anemometer.

[29]Corrections due to the compressibility of air are on the order of $(v/v_s)^2$, where v is the flow velocity and $v_s \simeq 340$ m/s the speed of sound in air. For our parameters, compressibility thus amounts to an error of about 1% at most, and is completely negligible with respect to other sources of uncertainty.

[30]B. Pelle, H. Bitard, G. Bailly, and C. Robilliard, "Magnetoelectric directional nonreciprocity in gas-phase molecular nitrogen," Phys. Rev. Lett. **106**, 193003 (2011).

[31]É. Guyon, J.-P. Hulin, L. Petit, C. D. Mitescu, *Physical Hydrodynamics* (Oxford U.P., Oxford, 2001).

[32]T. E. Faber, *Fluid Dynamics for Physicists* (Cambridge U.P., Cambridge, 1995).

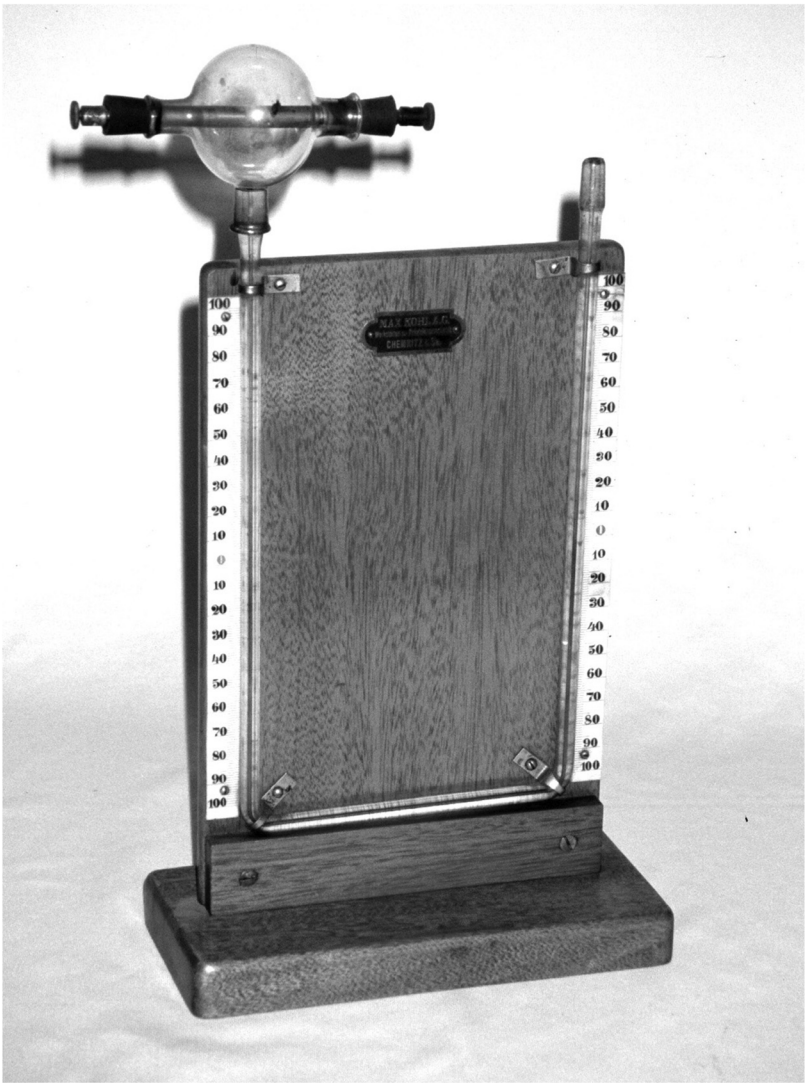

Heating Effects of an Electric Current. This piece of apparatus is at Case Western Reserve University in Cleveland, Ohio, and was made by Max Kohl of Chemnitz, Germany. It was used to demonstrate the heating effects of the electric current that passed through the conductor in the sealed glass bulb. The air in the bulb expanded, thus pushing the oil in the manometer down on the left-hand side. (Notes and photograph by Thomas B. Greenslade, Jr., Kenyon College)